Berod, L., Heinemann, C., Heink, S., Escher, A., Stadelmann, C., Drube, S., Wetzker, R., Norgauer, J., Kamradt, T.

PI3Kγ deficiency delays the onset of experimental autoimmune encephalomyelitis and ameliorates its clinical outcome

(2011) European Journal of Immunology, 41 (3), pp. 833-844

European Journal of Immunology

PI3Kγ deficiency delays the onset of experimental autoimmune encephalomyelitis and ameliorates its clinical outcome

Luciana Berod[1,2], Christina Heinemann[1], Sylvia Heink[1], Angelika Escher[3], Christine Stadelmann[3], Sebastian Drube[1], Reinhard Wetzker[4], Johannes Norgauer[2] and Thomas Kamradt[1]

[1] Institute for Immunology, University Hospital Jena, Friedrich-Schiller-University Jena, Jena, Germany
[2] Experimental Dermatology, University Hospital Jena, Friedrich-Schiller-University Jena, Jena, Germany
[3] Institute for Neuropathology, Georg-August University Göttingen, Göttingen, Germany
[4] Institute for Molecular Cell Biology, Center for Molecular Biomedicine, University Hospital Jena, Friedrich-Schiller-University Jena, Jena, Germany

PI3Ks control signal transduction triggered by growth factors and G-protein-coupled receptors and regulate an array of biological processes, including cellular proliferation, differentiation, survival and migration. Herein, we investigated the role of PI3Kγ in the pathogenesis of EAE. We show that, in the absence of PI3Kγ expression, clinical signs of EAE were delayed and mitigated. PI3Kγ-deficient myelin oligodendrocyte glycoprotein $(MOG)_{35–55}$-specific $CD4^+$ T cells appeared later in the secondary lymphoid organs and in the CNS than their WT counterparts. Transfer of WT $CD4^+$ cells into PI3K$\gamma^{-/-}$ mice prior to $MOG_{35–55}$ immunisation restored EAE severity to WT levels, supporting the relevance of PI3Kγ expression in Th cells for the pathogenesis of EAE; however, PI3Kγ was dispensable for Th1 and Th17 differentiation, thus excluding an altered expression of these pathogenetically relevant cytokines as the cause for ameliorated EAE in PI3K$\gamma^{-/-}$ mice. These findings demonstrate that PI3Kγ contributes to the development of autoimmune CNS inflammation.

Keywords: Autoimmune disease · EAE · PI3Kγ · T cells

Supporting Information available online

Introduction

EAE is an autoimmune disorder of the CNS that serves as an animal model for the human disease multiple sclerosis (MS) [1]. Both in MS and EAE, Th1 and Th17 myelin-reactive $CD4^+$ T lymphocytes gain access to the CNS and, in concert with other infiltrating mononuclear cells such as macrophages, cause inflammation, oligodendrocyte cell death, demyelination, axonal degeneration and progressive ascending paralysis [2–4].

PI3Kγ belongs to the Class IB family of dual-specificity lipid and protein kinases that catalyse the phosphorylation of phosphatidylinositol-4,5-biphosphate into the second messenger phosphatidylinositol-3,4,5-triphosphate [5, 6]. First characterised in the early 1990s, PI3Kγ is mainly expressed in blood and

Correspondence: Dr. Thomas Kamradt
e-mail: Immunologie@mti.uni-jena.de

endothelial cells [7] and is activated in response to most G-protein-coupled chemokine receptors [8, 9]. Thus, PI3Kγ regulates migration of different cell populations such as neutrophils, macrophages, DCs and T cells [10–14]. Recently, a role for PI3Kγ in regulating the in vivo migration of Ag-experienced effector $CD4^+$ T cells into inflammatory sites has been described previously [15]. Moreover, migration of Th17 cells in response to CCR2 and CCR6 agonists has been found to be PI3K dependent [16]. In addition, PI3Kγ has been involved in other inflammatory cellular processes such as superoxide production by neutrophils [17], NK cell cytotoxicity [18] and T-cell activation [19].

Recent studies have proposed PI3Kγ as a target for the treatment of inflammatory pathologies including asthma [20, 21], rheumatoid arthritis [22, 23], allergy [24–26], systemic lupus erythematosus [27] and pancreatitis [28, 29]. Yet, the function of PI3Kγ in EAE pathogenesis remains unclear. Here, we investigated the effect of PI3Kγ deletion on the course of chronic EAE and its influence on the immune mechanisms underlying pathogenesis.

Results

Late onset and reduced severity of EAE in PI3Kγ$^{-/-}$ mice

Following s.c. immunisation with myelin oligodendrocyte glycoprotein $(MOG)_{35–55}$ peptide in CFA and administration of pertussis toxin i.v., WT mice reproducibly developed a severe, chronic encephalomyelitis with clinical signs of disease appearing between days 13 and 19 post-immunisation (pi) (Fig. 1A). The onset of clinical symptoms in PI3Kγ$^{-/-}$ mice was delayed by approximately 10 days compared with the WT mice (Fig. 1A and Table 1). Disease severity, as judged by the maximal and cumulative clinical scores, was significantly lower in PI3Kγ$^{-/-}$ mice (Table 1). Reduced severity was also revealed by the reduced body weight loss that PI3Kγ$^{-/-}$ mice experienced during the symptomatic phase of EAE when compared with WT mice (Fig. 1B). Moreover, although more than 90% of the WT mice reached scores ≥ 3, less than 50% of the PI3Kγ$^{-/-}$ mice developed a complete hind leg paralysis (score = 3) (Fig. 1C), which mostly improved within 24 h. In addition, although approximately 30% of the WT mice died, survival in PI3Kγ$^{-/-}$ mice was 100% in all experiments performed (Table 1). Thus, both EAE incidence and mortality were lower in PI3Kγ$^{-/-}$ than in WT mice, suggesting that PI3Kγ might be important for EAE onset as well as for its clinical outcome.

To characterise disease progression at the level of tissue damage, CNS inflammatory lesions during the symptomatic phase of EAE (day 16 pi) were examined in WT and PI3Kγ$^{-/-}$ mice. WT mice with acute symptoms of EAE (score ≥ 3) presented abundant cell infiltrates dominated by macrophages and T cells including some neutrophils (Fig. 1D, i–iv). Demyelinating lesions, as assessed by Luxol fast blue (LFB) staining, were present in the spinal cord and absent in the brain (Fig. 1D-i, and data not shown). On the contrary, at day 16, PI3Kγ$^{-/-}$ mice showed minimal or absent spinal cord inflammatory infiltrates (Fig. 1D, v–viii).

Delayed immune response in the peripheral lymphoid organs of PI3Kγ$^{-/-}$ mice

To gain mechanistic insights into the effects of PI3Kγ deficiency during EAE, draining lymph nodes (dLN) and spleens from mice were removed before immunisation and on days 9 and 15 after $MOG_{35–55}$ immunisation. Absolute cell numbers were determined and in vitro recall assays were performed to examine cytokine production and Ag-specific proliferation. Before immunisation, total cell counts were similar in the secondary lymphatic organs from PI3Kγ$^{-/-}$ mice and WT controls (Fig. 2A). On the contrary, during the induction phase of EAE (day 9) when neither WT nor PI3Kγ$^{-/-}$ mice displayed clinical signs of disease, total cell numbers were significantly lower in PI3Kγ$^{-/-}$ spleen and dLN compared with WT controls (Fig. 2A). At day 15 pi, when WT but not PI3Kγ$^{-/-}$ mice already displayed severe signs of EAE (score ≥ 3), total cell numbers in the dLN of WT mice were slightly decreased compared with day 9 pi. Cellularity in the spleen of WT mice at this time point was approximately half of the total cell numbers compared with day 9 pi (Fig. 2A, black bars). On the contrary, total cell numbers in dLN and spleens of PI3Kγ$^{-/-}$ mice were slightly increased compared with day 9 pi (Fig. 2A, grey bars). At day 15 pi, total cell numbers in spleens of PI3Kγ$^{-/-}$ mice were significantly higher than in their WT counterparts (Fig. 2A).

Proliferation was evaluated in total dLN cells and splenocytes after in vitro re-stimulation for 72 h. At day 9 pi, splenocytes and dLN cells from PI3Kγ$^{-/-}$ mice showed significantly lower proliferation than WT controls when re-stimulated in the presence of MOG peptide (Fig. 2B). Proliferation in response to the cognate Ag at day 15 pi reached a similar magnitude in both PI3Kγ$^{-/-}$ and WT dLN and spleens (data not shown).

Culture supernatants from PI3Kγ$^{-/-}$ splenocytes or dLN obtained at day 9 pi and stimulated in vitro with $MOG_{35–55}$ contained less IFN-γ and IL-17A than the supernatants from WT controls (Fig. 2C and data not shown). However, at day 15 pi, production of IFN-γ and IL-17A was similar in splenocytes and dLN cells of PI3Kγ$^{-/-}$ and WT mice, respectively (Fig. 2C).

$MOG_{35–55}$ Ag-specific Th cells appear later in PI3Kγ$^{-/-}$ mice

DCs obtained from PI3Kγ$^{-/-}$ mice have a reduced ability to respond to chemokines in vitro and ex vivo and to travel to dLN under inflammatory conditions [10]. Therefore, we hypothesised that activation of encephalitogenic $CD4^+$T cells by DCs in the lymphoid organs of PI3Kγ$^{-/-}$ mice might be delayed in comparison with WT mice. To test this, polychromatic flow cytometry was used to compare the MOG-specific $CD4^+$ Th-cell response in PI3Kγ$^{-/-}$ and WT mice. Spleen and dLN cells from

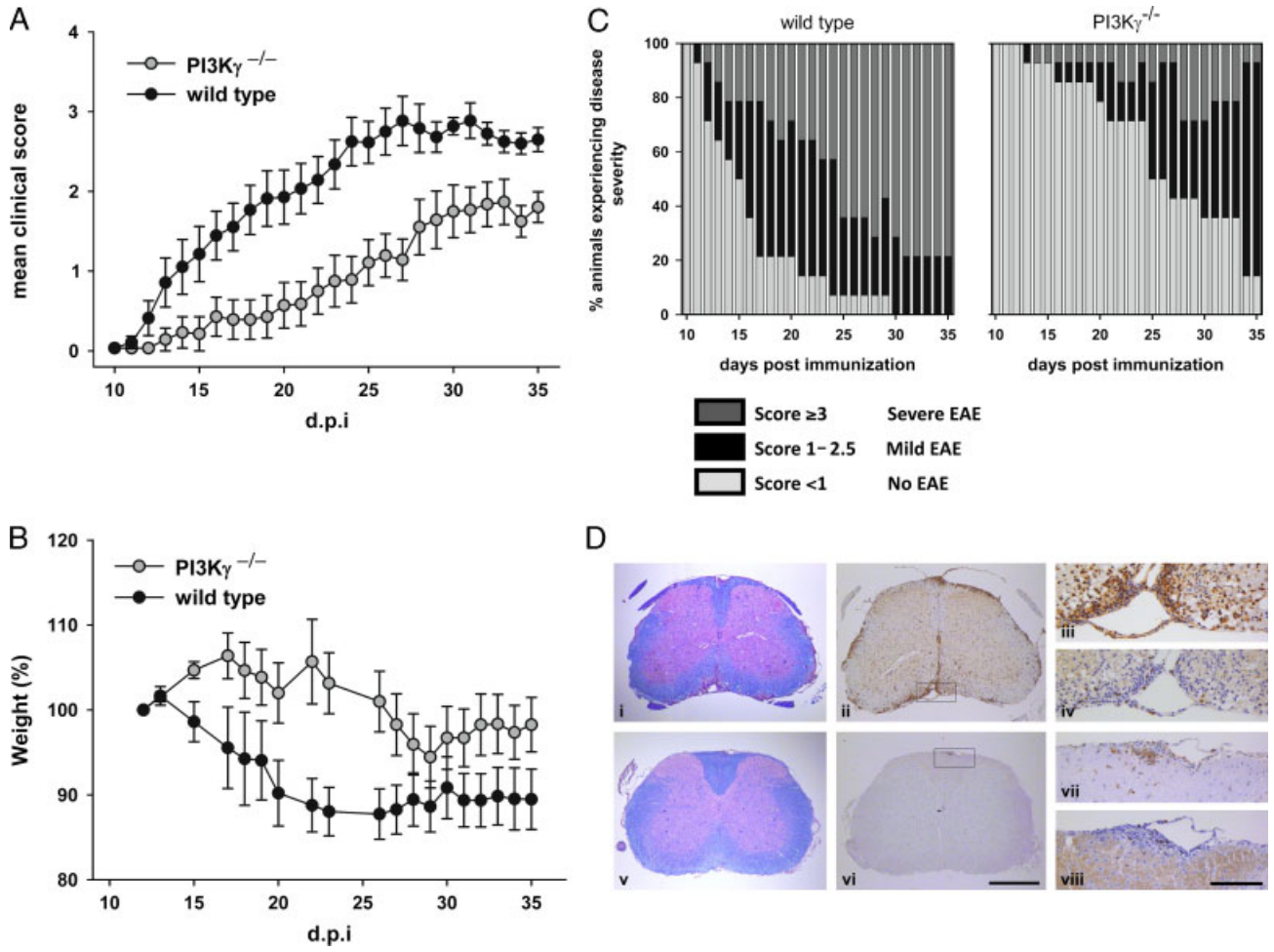

Figure 1. Late onset and reduced severity of EAE in PI3Kγ-deficient mice. EAE was induced in WT ($n = 14$) and PI3K$\gamma^{-/-}$ mice ($n = 14$) and disease progression was evaluated. (A) EAE clinical score of WT (black circles) and PI3K$\gamma^{-/-}$ (grey circles) mice. (B) Loss of body weight calculated as percentage of the weight at day 10 pi. Data show mean ± SEM (A and B). (C) Distribution of disease severity expressed as the percentage of mice with severe (score ≥3), mild (score ≤2.5 and ≥1) or no EAE (score <1) at each time point. Results shown are cumulative of three experiments. (D) Histology and immunohistochemistry of spinal cord sections from WT (i–iv) and PI3K$\gamma^{-/-}$ (v–viii) mice with clinical scores of 3 and 0.5, respectively, collected on day 16 pi [i, v: LFB/PAS (myelin and inflammatory infiltrates); ii, iii, vi, vii: Mac-3 (activated microglia and macrophages), iv, viii: $CD3^+$ T cells]. Panels iii, iv and vii, viii represent the lesion areas delineated in ii and vi, respectively. Scale bars: i, ii, v, vi: 500 μm (original magnification: ×40); iii, iv, vii, viii: 100 μm (×200).

Table 1. Summary of EAE clinical parameters[a)]

Group	Incidence	Mortality	Day of onset[b)]	Maximum clinical score[b)]	Cumulative clinical score[b) c)]
WT	14/14 = 100%	4/14(29%)	16.4 ± 1.4	3.7 ± 0.3	53.5 ± 5.3
PI3K$\gamma^{-/-}$	12/14 = 86%	0/14(0%)	25.5 ± 2.1**	2.4 ± 0.2***	23.3 ± 4.7***

[a)] Cumulative results from three experiments.
[b)] *$p \leq 0.05$, **$p \leq 0.01$ and ***$p \leq 0.001$ calculated by Mann–Whitney *U*-rank sum test.
[c)] Cumulative clinical score calculated over the first 35 days.

PI3K$\gamma^{-/-}$ and WT mice were prepared at different time points after immunisation, briefly re-stimulated with $MOG_{35–55}$, fixed and stained for the effector cytokines IFN-γ, TNF-α, IL-17A and IL-2 as described in Materials and methods section and detailed in our previous studies [30, 31]. $MOG_{35–55}$-specific T cells were identified by staining simultaneously for CD4 and CD154 (CD40L) (Supporting Information Fig. S1A). CD154 is up-regulated within a few hours after TCR triggering and has been previously shown to be induced only in those T cells that have recognised their cognate Ag [32–35] (and own unpublished data). At day 10 pi, MOG-specific Th cells that produced IL-17A (1%), IFN-γ (1%), TNF-α (1.6%) or IL-2 (1.5%) were detectable in the dLN of WT but not PI3K$\gamma^{-/-}$ mice (Fig. 3A left upper panel, Supporting Information Fig. S1B and data not

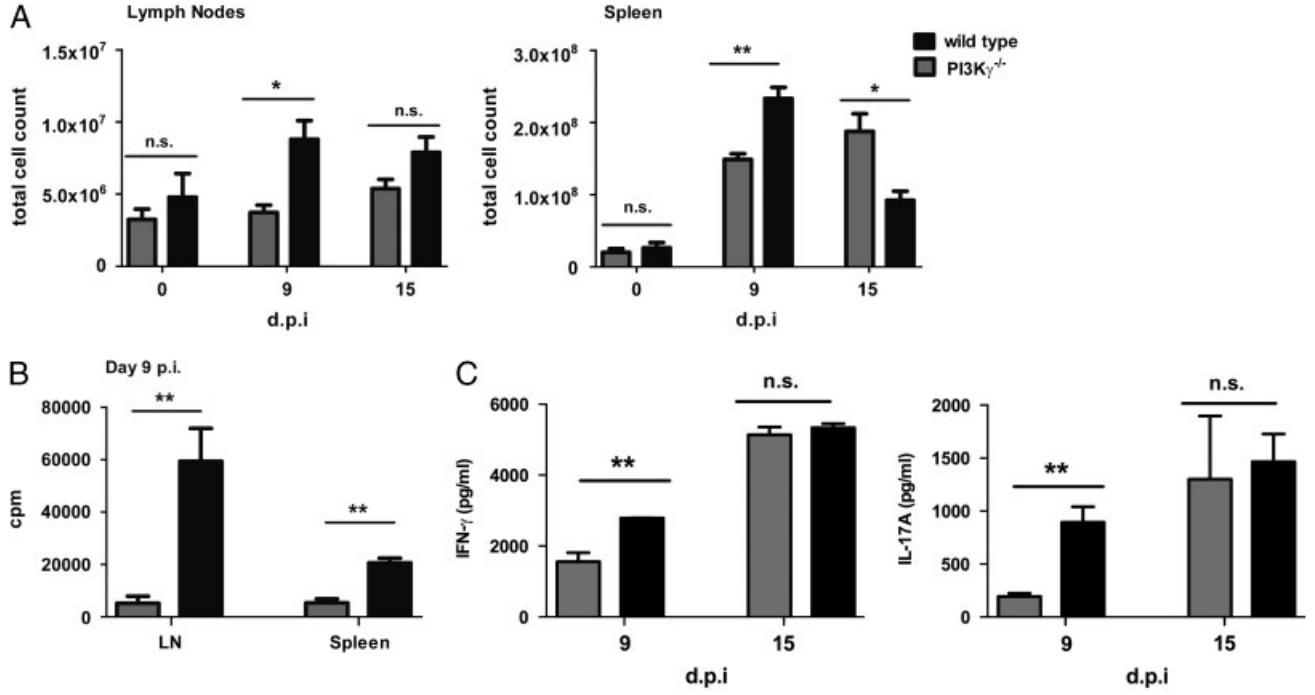

Figure 2. Delayed immune response in the peripheral lymphoid organs of PI3K$\gamma^{-/-}$ mice. WT or PI3K$\gamma^{-/-}$ mice were immunised with MOG_{35-55} or left untreated and on days 0, 9 and 15 pi, spleen and dLN (aortic, inguinal) were collected. (A) Total cell numbers in dLN (left panel) and spleen (right panel) from WT (black) and PI3K$\gamma^{-/-}$ (grey) mice. (B) In vitro proliferation of dLN or splenocytes at day 9 pi determined after re-stimulation with MOG_{35-55} for 72 h. (C) Cytokine concentration determined by ELISA in supernatants from splenocytes cultured for 48 h in the presence of MOG_{35-55} peptide. Data show mean+SEM ($n = 3$–5 mice per group). Results are representative of at least two independent experiments (n.s., not significant, $^{*}p \leq 0.05$, $^{**}p \leq 0.01$).

shown). Similarly, although approximately 1.5% of the splenic $CD4^+$ cells produced IL-17A or IFN-γ upon recognition of their cognate MOG peptide, such MOG-specific cytokine producers were barely detectable only in the spleens of PI3K$\gamma^{-/-}$ mice (Fig. 3A, left lower panel). Similar results were observed for TNF-α (2.2 versus 0.2%) or IL-2 (1.7 versus 0.3%) in WT and PI3K$\gamma^{-/-}$ mice, respectively (data not shown).

Sixteen days after immunisation, the percentage of MOG-specific Th cells that produced IL-17A or IFN-γ in the dLN had already decreased in the WT mice (Fig. 3A right upper panel and Supporting Information Fig. S1B). At this time point, a sizeable fraction of Th cells in the dLN of PI3K$\gamma^{-/-}$ mice produced IFN-γ (0.6%), IL-17A (0.5%), TNF-α (1.8%) or IL-2 (1.7%) (Fig. 3A right upper panel and data not shown). Thus, the frequency of MOG-specific cytokine producers was similar in the spleens of WT and PI3K$\gamma^{-/-}$ mice. Collectively, these data are compatible with the concept that priming of MOG-specific Th cells in the secondary lymphoid organs upon immunisation is delayed in PI3K$\gamma^{-/-}$ mice.

To determine whether the lower percentage of cytokine-producing $CD4^+$ T cells in PI3K$\gamma^{-/-}$ mice at early time points was accompanied by an impaired expansion of the MOG-specific T-cell population, absolute numbers of $CD4^+CD154^+$ T cells were calculated. In WT inguinal and aortic LN, the number of Ag-specific Th cells increased after day 6 and reached its maximum on day 21 pi (Fig. 3B, upper panel). MOG-specific $CD4^+$ T cells became detectable at day 13 in PI3K$\gamma^{-/-}$ dLN, increased thereafter until day 21 pi. In WT spleens, the size of the $CD4^+$ $CD154^+$ T-cell pool expanded progressively peaking at day 13 pi when the number of Ag-specific T cells was ten times higher than at day 3 pi (Fig. 3B, left lower panel). Thereafter, the number of MOG-specific Th cells in the spleens of WT mice decreased, probably reflecting cell migration to the CNS (Fig. 3B left upper panel). WT mice at this time point had clinical EAE scores of 3 and inflammatory infiltrates into the CNS.

In PI3K$\gamma^{-/-}$ spleens, the number of MOG-specific cells at day 3 pi was only half of the number found at the same time point in WT mice (Fig. 3B, left lower panel). In these mice, the number of MOG-specific T cells rose first between day 10 and day 13 pi and reached a peak at day 17 pi, but the absolute numbers were still lower than in WT spleens at day 13 pi.

Thus, by day 10 pi the number of MOG-specific Th cells in the secondary lymphatic organs is much higher in WT than in PI3K$\gamma^{-/-}$ mice (Fig. 3B). Moreover, within this larger pool of MOG-specific Th cells in WT mice, the relative frequency of cytokine producers is at least ten-fold higher than in their PI3K$\gamma^{-/-}$ counterparts (Fig. 3A), resulting in >100-fold higher numbers of cytokine-producing MOG-specific Th cells 10 days after immunisation in WT mice. Seventeen days after immunisation, both the numbers of MOG-specific Th cells (Fig. 3B) and the frequency of cytokine producers among them are similar in PI3K$\gamma^{-/-}$ and WT mice. Taken together, these data imply a retarded priming of Ag-specific Th cells in the PI3K$\gamma^{-/-}$ mice upon immunisation with MOG peptide.

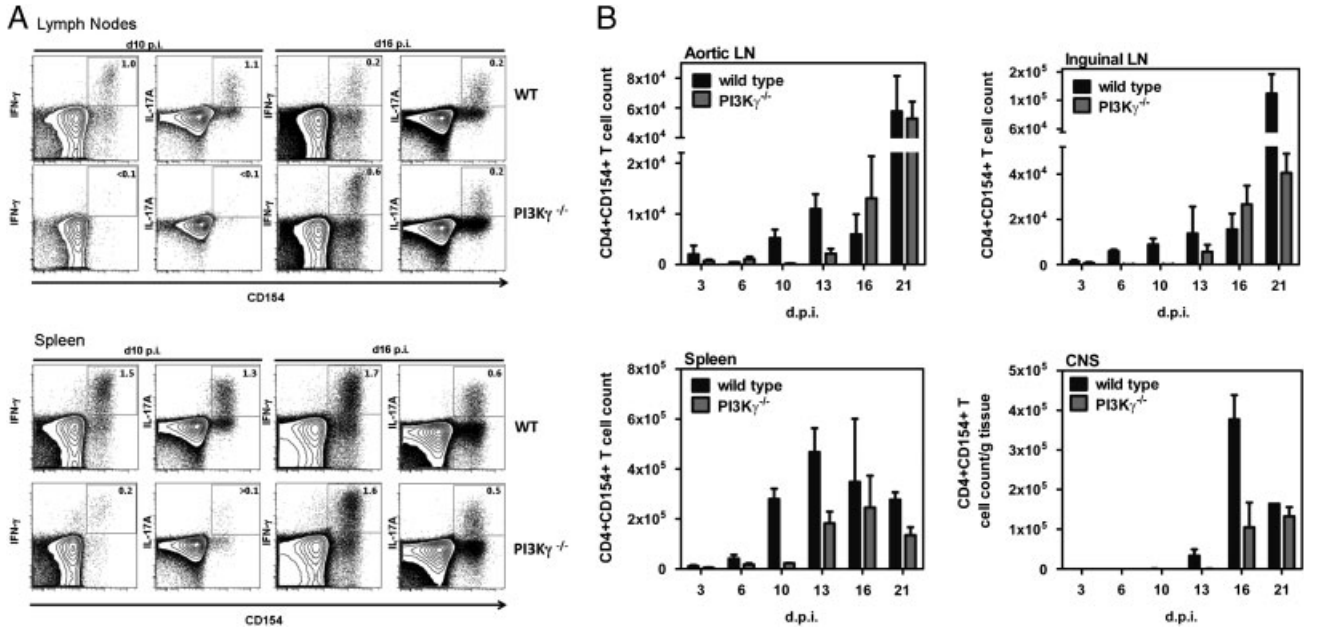

Figure 3. Late emergence of $MOG_{35–55}$-specific Th cells in PI3K$\gamma^{-/-}$ mice during EAE. Mice were immunised with $MOG_{35–55}$ and on days 10 and 16 pi, spleen and dLN were collected and briefly re-stimulated with $MOG_{35–55}$ as described in Materials and methods section. (A) Intracellular staining for IFN-γ and IL-17A. Contour plots show the expression of these cytokines in Ag-specific T cells (gated on $CD4^+$ as shown in Supporting Information Fig. S1A). Numbers in quadrants indicate the percentage of cells producing the respective cytokines within the Ag-specific T-cell compartment (shown in Supporting Information Fig. S1B). Data shown are from concatenated data files from three individual mice per group and represent all mice in the respective group. Data are representative of at least two independent experiments. (B) Total numbers of Ag-specific $CD4^+$ Th cells according to intracellular $MOG_{35–55}$-induced CD154 expression in para-aortic LN (upper left), inguinal LN (upper right), spleens (lower left) or brain and spinal cord mononuclear infiltrates (lower right) in WT (black bars) and PI3K$\gamma^{-/-}$ (grey bars) mice. Total numbers of $CD4^+CD154^+$ Th cells were calculated from the total cell count after FACS analysis. Data show mean+SEM ($n = 3$–4 mice/time point). Results are representative of two independent experiments.

Recently, it has been shown that PI3Kγ regulates the in vivo migration of Ag-experienced effector $CD4^+$ T lymphocytes into inflammatory sites during adaptive immune responses [15]. Moreover, migration of Th17 cells has been found to be PI3K dependent [16]. To assess whether $MOG_{35–55}$-specific T cells were able to reach the CNS in the absence of PI3Kγ expression, total lymphocytes from the brains and spinal cords of WT and PI3K$\gamma^{-/-}$ mice were isolated at different time points after EAE induction. After in vitro re-stimulation with $MOG_{35–55}$, the number of $CD4^+CD154^+$ T cells was determined by FACS. At day 9 pi, when still no signs of EAE were observed, $CD4^+CD154^+$ $MOG_{35–55}$-specific Th cells were almost undetectable in the CNS of WT and PI3K$\gamma^{-/-}$ mice (Fig. 3B, right lower panel). In WT mice, numbers of $CD4^+CD154^+$ Ag-specific Th cells in the CNS increased thereafter, reaching a peak at day 16 pi, concurrent with severe hind leg paralysis in WT mice. Contrastingly, in the CNS from PI3K$\gamma^{-/-}$ mice only few $MOG_{35–55}$-specific Th cells were found on day 16 pi and their numbers remained lower than in WT mice even at day 21 pi when PI3K$\gamma^{-/-}$ mice already displayed signs of disease. Thus, correlating with the later onset of clinical signs in PI3K$\gamma^{-/-}$ mice, infiltration or expansion of myelin-specific T cells occurs later and to a lesser extent both in the secondary lymphoid organs and in the CNS of PI3K$\gamma^{-/-}$ mice than in WT controls.

Inflammatory lesions occur later in the CNS of PI3K$\gamma^{-/-}$ mice

In addition to $CD4^+$ T cells, other cell populations infiltrate and contribute to tissue injury during EAE. To obtain a more complete picture, cell infiltrates in the CNS of PI3K$\gamma^{-/-}$ mice and WT littermates were analysed at different time points during disease. As expected, at day 16 pi cell infiltration into the CNS of non-symptomatic PI3K$\gamma^{-/-}$ mice was significantly lower than in WT mice that had already developed severe signs of EAE, correlating with our immunohistochemistry studies (Fig. 1D and data not shown). However, when infiltrates in the CNS of WT or PI3K$\gamma^{-/-}$, mice were compared at the peak of disease (days 21–25 pi) with average scores of 3.1 ± 0.4 and 2.7 ± 0.1, respectively, with the exception of $CD3^+$ $CD8^+$ cells, no differences in the percentages or absolute numbers of $CD3^+CD4^+$, NK cells, neutrophils, monocytes or B cells were observed (Fig. 4A and Supporting Information Fig. S2). Thus, PI3Kγ deficiency delays but does not prevent inflammatory infiltrates in the CNS.

To determine whether cellular infiltration was similar in terms of spatial distribution, the CNS from WT and PI3K$\gamma^{-/-}$ mice was examined by immunohistochemistry. Inflammatory infiltrates were found in the meninges and sub-pial white matter in sections analysed from WT and PI3K$\gamma^{-/-}$ mice. PI3K$\gamma^{-/-}$, but not WT

mice, showed prominent brain stem involvement (Fig. 4B and data not shown). At day 28 pi, infiltrates in PI3K$\gamma^{-/-}$ presented substantial PMN, reflecting early lesions (Fig. 4B, i–v). However, comparing PI3K$\gamma^{-/-}$ (Fig. 4B, i-v) and WT mice (Fig. 4B, v–xi) at early time points of lesion formation (day 28pi for PI3K$\gamma^{-/-}$ and day 16pi for WT mice), a similar extent of spinal inflammatory infiltration (Fig. 4B, i, vi) and comparable levels of macrophage infiltration/microglia activation (Fig. 4B, ii, iii, vii, viii), CD3$^+$ T cells (Fig. 4B, iv, ix) and neutrophilic granulocytes (Fig. 4B, v, x) were observed.

Transfer of WT CD4$^+$ Th cells into PI3K$\gamma^{-/-}$ mice increases disease severity

The reduced number of MOG-specific Th cells in infiltrating the CNS and the less severe EAE in PI3K$\gamma^{-/-}$ mice could have been due to T-cell intrinsic factors such as an impaired migration capacity of CD4$^+$ effector T cells, but also to T-cell extrinsic factors, such as abnormal presentation of the MOG_{35-55} peptide. To distinguish between these possibilities, syngenic PI3K$\gamma^{+/+}$ CD4$^+$ Th cells were adoptively transferred into PI3K$\gamma^{-/-}$ mice.

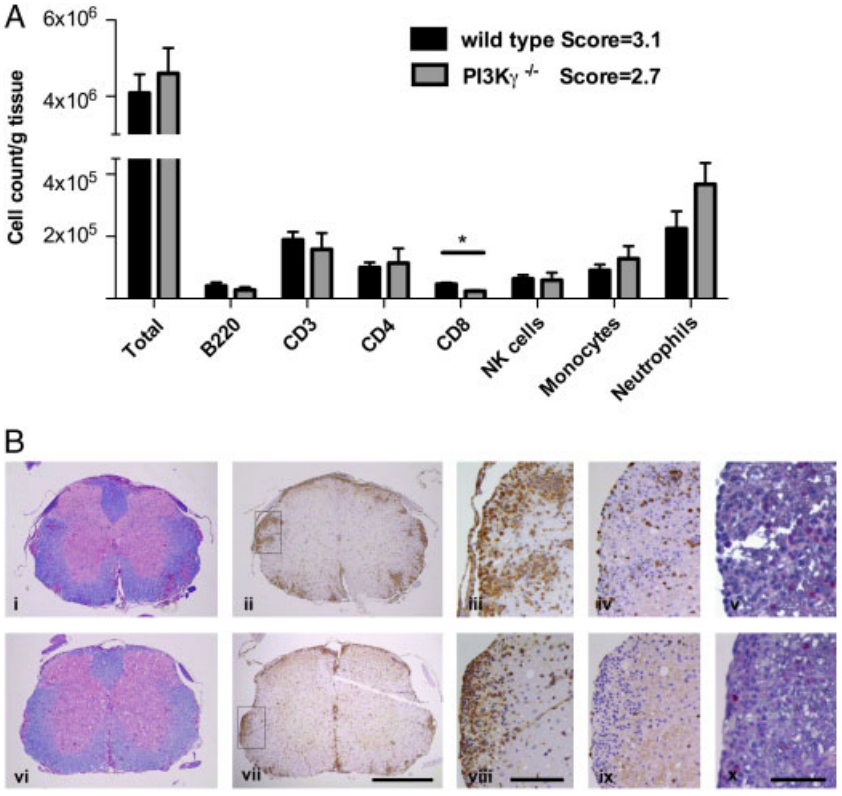

Figure 4. Infiltration of effector cells into the CNS of PI3K$\gamma^{-/-}$ mice correlates with clinical onset. (A) Total number of CD3$^+$, CD3$^+$CD4$^+$, CD3$^+$CD8$^+$, B220$^+$, NK/NK-T cells, CD45^{high}CD11b$^+$Ly6C^{int}Gr-1$^+$ neutrophils or CD45^{high}CD11b$^+$Ly6C^{high}F4/80$^+$ monocytes in brain and spinal cord infiltrates from WT and PI3K$\gamma^{-/-}$ mice calculated from the total cell count after FACS analysis (gated as shown in Supporting Information Fig. S2). Data show mean+SEM ($n = 4$) (*$p \leq 0.05$). Results are representative of two independent experiments. (B) Inflammatory infiltration in PI3K$\gamma^{-/-}$ (i–v) and WT (vi–x) mice at the peak of disease. [i, vi: LFB/PAS (myelin and inflammatory infiltrates); ii, iii, vii, viii: Mac-3; iv, ix: CD3$^+$ T cells; v, x: chloroacetate stearase enzyme, red (neutrophilic granulocytes)]. Panels iii–v and viii–x represent the lesion areas delineated in ii and vii, respectively. Scale bars: i, ii, vi, vii: 500 μm (original magnification: ×40); iii, iv, viii, ix: 100 μm (×200), v, x: 50 μm (×400). Results are representative of two to three mice/group.

Table 2. Summary of EAE clinical parameters[a)]

Group	Incidence	Mortality	Day of onset[b)]	Maximum clinical score[b)]
WT	13/13 = 100%	6/13 (46%)	14.3±0.5	3.7±0.2
PI3K$\gamma^{-/-}$	7/10 = 70%	0/10 (0%)	18.4±1.5*	2.3±0.4**
PI3K$\gamma^{-/-}$+PI3K$\gamma^{+/+}$ CD4$^+$ T cells	7/7 = 100%	1/10 (10%)	19.3±1.6*	3.2±0.1*
WT+PI3K$\gamma^{-/-}$CD4$^+$ T cells	7/7 = 100%	4/7(57%)	13.5±0.5	3.6±0.2

[a)]Results are representative of at least two experiments.
[b)]*$p \leq 0.05$ and **$p \leq 0.01$ calculated by Mann–Whitney *U*-rank sum test.

WT mice that received PI3K$\gamma^{-/-}$CD4$^+$Th cells or no cells were used as controls. After 4 days, PI3K$\gamma^{-/-}$ and WT mice were immunised with MOG_{35-55} in CFA and the clinical course of the disease was evaluated. Although transfer of PI3K$\gamma^{+/+}$CD4$^+$ Th cells into PI3K$\gamma^{-/-}$ mice sometimes resulted in an earlier onset of the disease compared with PI3K$\gamma^{-/-}$ mice, the average clinical onset was still delayed when compared with WT controls that received or not, PI3K$\gamma^{-/-}$CD4$^+$ Th cells (Table 2). Disease severity was comparable in PI3K$\gamma^{-/-}$ mice that received PI3K$\gamma^{+/+}$CD4$^+$ T cells and WT animals with or without PI3K$\gamma^{-/-}$CD4$^+$ Th cells. On the contrary, PI3K$\gamma^{-/-}$ mice showed a reduced severity and recovered faster after reaching a maximal score of 3. Thus, the presence of WT CD4$^+$ T cells expressing PI3Kγ was enough to trigger severe EAE symptoms in PI3Kγ-deficient mice, whereas it did not affect the onset of the disease, suggesting the additional involvement of other mechanisms.

To determine whether WT transferred CD4$^+$ T cells or PI3K$\gamma^{-/-}$ endogenous T cells were present in the CNS of PI3K$\gamma^{-/-}$ mice, WT Ly5.1$^+$ Th cells were adoptively transferred into Ly5.2$^+$ recipients that were either WT or PI3Kγ-deficient. Confirming our earlier results (Table 2), the WT mice but not the PI3K$\gamma^{-/-}$ mice that had received WT Th cells showed a severe EAE by day 15 pi (Fig. 5A). Moreover, at this time point, both endogenous Ly5.1$^-$ and transferred Ly5.1$^+$MOG-specific Th cells were present in the CNS of the diseased WT mice in similar frequencies (Fig. 5B, upper panel and Supporting Information Fig. S3B). On the contrary, the vast majority of the MOG-specific Th cells isolated from the CNS of the only moderately ill PI3K$\gamma^{-/-}$-deficient mice were Ly5.1$^+$ WT donor cells with only very few endogenous Ly5.1$^-$ PI3K$\gamma^{-/-}$ MOG-specific Th cells (Fig. 5C and Supporting Information Fig. S3B, left panel). Three wk after immunisation, when PI3K$\gamma^{-/-}$ mice had developed a more severe EAE, the majority of the MOG-specific Th cells isolated from the CNS were endogenous Ly5.1$^-$ PI3Kγ-deficient Th cells (Fig. 5B, lower panel, Fig. 5C and Supporting Information Fig. S3B, right panel). Thus, the data indicate that during EAE, MOG-specific WT Ly5.1$^+$Th cells reach the CNS of PI3K$\gamma^{-/-}$ mice earlier (d15) than the endogenous (Ly5.1$^-$) MOG-specific PI3Kγ-deficient Th cells.

PI3Kγ is dispensable for the differentiation of naïve T cells into Th1 and Th17 cells

Since cell infiltration into the CNS, although later, was comparable in PI3K$\gamma^{-/-}$ and WT mice with severe symptoms of EAE, we hypothesised that the less severe form observed in these mice might be a result of other effector mechanisms affected by PI3Kγ deficiency. Several studies indicate that both Th1- and Th17 CD4$^+$-mediated cell responses are critical in the pathogenesis of EAE [36, 37]. DCs instruct Th-cell differentiation in vivo and

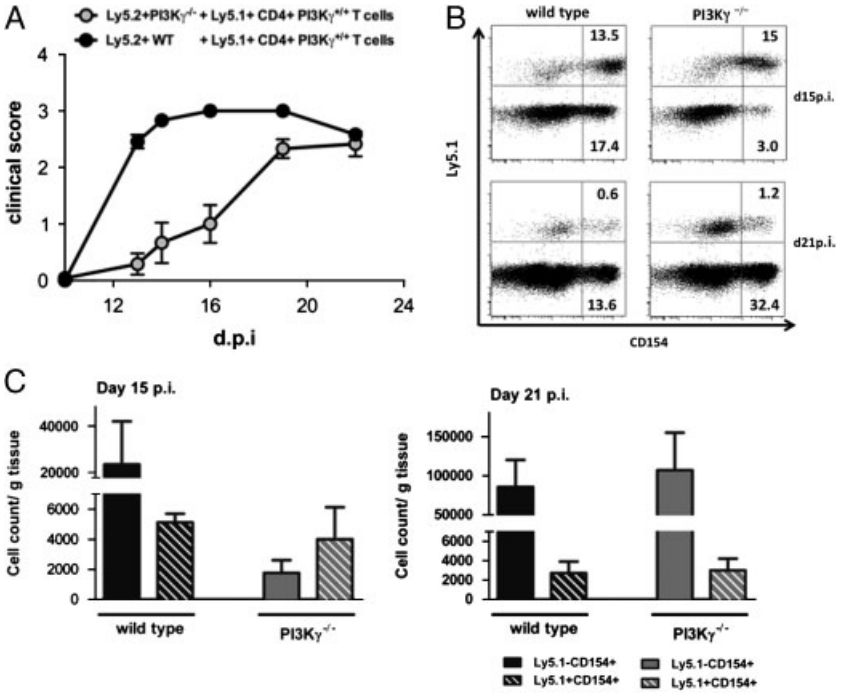

Figure 5. Transfer of WT CD4$^+$ Th cells into PI3K$\gamma^{-/-}$ mice influences disease severity but not clinical onset. Ly5.1 congenic PI3K$\gamma^{+/+}$CD4$^+$CD62L$^+$ T cells were adoptively transferred into Ly5.2 WT and PI3K$\gamma^{-/-}$ mice. After 4 days, PI3K$\gamma^{-/-}$ and WT mice were immunised with MOG_{35-55} in CFA and (A) the clinical course of the disease was evaluated. (B) Frequency and (C) Total cell number of Ag-specific CD4$^+$ Th cells according to intracellular MOG_{35-55}-induced CD154 expression in CNS of PI3K$\gamma^{-/-}$ and WT at days 15 and 21 pi (gates and summarizing bar graphs are shown in Supporting Information Fig. S3A and B). Data show mean $\pm$ SEM (n = 3 mice/group). Data shown are from one of the two independent experiments.

in vitro. Therefore, the influence of PI3Kγ deficiency in BMDC and naïve T cells to drive Th cell differentiation was next investigated. Naïve $CD4^+CD62L^+$ Th cells were purified from the spleens and LNs of WT and PI3K$\gamma^{-/-}$ mice and cultured with WT or PI3K$\gamma^{-/-}$ BMDC under Th0, Th1 or Th17 polarizing conditions. After 7 days, cells were re-stimulated for 4 h with PMA/ionomycin and assessed for their expression of IL-17A, TNF-α or IFN-γ by intracellular staining and FACS. No differences in the percentages of IFN-γ-, TNF-α- or IL-17A-producing cells were observed between WT and PI3K$\gamma^{-/-}$ $CD4^+$ T cells (Fig. 6, Supporting Information Fig. S4 and data not shown). A lower but not significant percentage of IFN-γ-producing cells was detected when $CD4^+$ WT or PI3K$\gamma^{-/-}$ T cells were cultured in the presence of PI3K$\gamma^{-/-}$ BMDC under Th1 conditions. Therefore, PI3Kγ deficiency did not affect the capacity of naïve T cells to differentiate into Th1 or Th17 cells in vitro.

Treatment of EAE by blockade of PI3Kγ activity

Given the lower severity of EAE found in PI3K$\gamma^{-/-}$ mice, we next determined whether pharmacological inhibition of the PI3Kγ catalytic activity in WT animals would also affect EAE development. WT mice received PI3Kγ inhibitor i.p. starting after the onset of clinical symptoms on day 13 pi with $MOG_{35–55}$ peptide. Milder signs of the disease and reduced body weight loss (Fig. 7A and B) were observed in mice treated with PI3Kγ inhibitor compared with mice treated with vehicle although to a lesser extent than in PI3K$\gamma^{-/-}$ mice.

Discussion

In the present study, we investigated the effect of PI3Kγ deficiency on the pathogenesis of EAE. We show that in PI3K$\gamma^{-/-}$ mice, clinical signs of EAE developed slower and were less severe than in WT controls. During the first 10 days after immunization, the number of MOG-specific Th cells was drastically lower in the secondary lymphatic organs of PI3K$\gamma^{-/-}$ mice than in WT mice. In addition, within this smaller pool of MOG-specific Th cells, the percentage of cytokine producers was much lower in PI3K$\gamma^{-/-}$ mice than in WT. At day 16 pi, both the numbers of MOG-specific Th cells and the percentage of cytokine producers within the MOG-specific Th cell pool were similar in the secondary lymphatic organs of PI3K$\gamma^{-/-}$ mice and in WT mice.

Upon Ag exposure, migration of Ag carrying DCs to the secondary lymphoid organs is a prerequisite for the activation of naïve T cells. Thus, DC migration represents a critical step to trigger an optimal immune response. Previous studies have demonstrated that PI3Kγ plays a non-redundant role in DC trafficking and T-cell activation [10]. DCs from PI3K$\gamma^{-/-}$ mice have a reduced ability to respond to chemokines in vitro and ex vivo and to travel to dLN under inflammatory conditions [10]. Importantly, this reduced ability of Ag-loaded DCs to migrate from the periphery to dLN results in impaired delayed-type hypersensitivity reactions in PI3K$\gamma^{-/-}$ mice [10]. Pertinent to our study, Del Prete et al. also found that although DCs from PI3K$\gamma^{-/-}$ mice had an impaired capacity to travel to the dLN, they localised to the T-cell paracortical areas just as WT DCs once

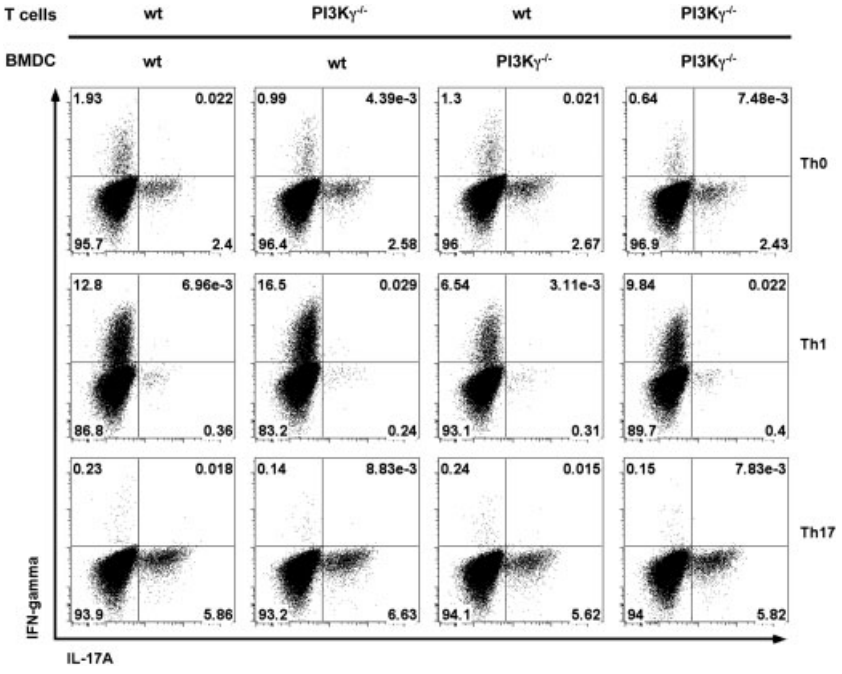

Figure 6. Differentiation of naïve T cells into Th subsets is not affected by PI3Kγ deficiency. In vitro differentiation of MACS sorted $CD4^+CD62L^+$ naïve T cells incubated under Th0, Th1 or Th17 polarizing conditions as described in Materials and methods section. After stimulation, cells were fixed and intracellularly stained for FACS analysis. Cytokine production by $CD4^+$ live T cells is shown (gated as shown in Supporting Information Fig. S1A). Bar graph summarizing data from three independent experiments is shown in Supporting Information Fig. S4.

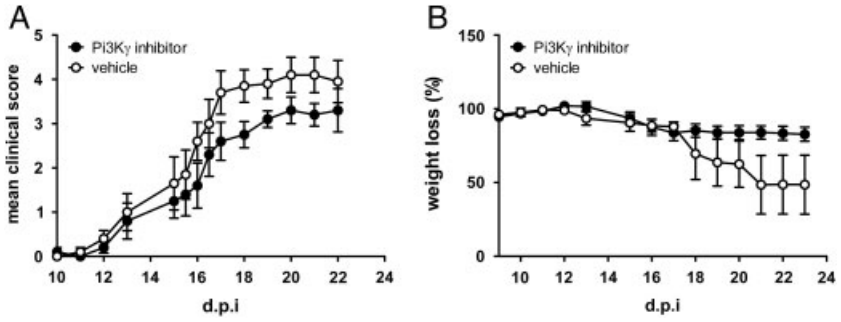

Figure 7. Pharmacological inhibition of PI3Kγ ameliorates EAE. (A) Mean clinical score and (B) weight loss (represented as a percentage of the weight at day 0) in PI3Kγ$^{+/+}$ mice treated with vehicle ($n = 5$) or 30 mg/Kg PI3Kγ inhibitor ($n = 5$) i.p. after onset of clinical symptoms. Data are presented show mean ± SEM. Data shown represents one experiment.

they had reached the LN [10]. These findings complement our analyses of Th-cell responses following MOG immunisation. Collectively, our findings and those reported by Del Prete and colleagues strongly suggest that the lack of PI3Kγ delays T-cell priming in the secondary lymphoid organs, thus prolonging the induction phase, and consequently, the clinical onset of disease. Moreover, PI3Kγ$^{-/-}$ T cells have been reported to exhibit dramatic defects in their ability to traffic to peripheral inflammatory sites in vivo [15]. This functional deficiency is likely to contribute to the delayed onset of EAE in the PI3Kγ$^{-/-}$ mice.

In addition to the late onset of EAE, we have demonstrated that disease severity was also reduced in PI3Kγ$^{-/-}$ mice compared with their WT counterparts. Our transfer experiments showed that although WT CD4$^+$ T cells alone were not sufficient to accelerate EAE onset in PI3Kγ$^{-/-}$ mice, disease severity in PI3Kγ$^{-/-}$ mice that received WT CD4$^+$ T cells was comparable to WT mice. Once activated in the secondary lymphoid organs, migration of autoreactive CD4$^+$ T cells into the CNS represents a critical pathogenic event in the initiation of CNS inflammation [4, 38]. Analysis of cellular infiltrates in the CNS revealed that $MOG_{35–55}$-specific CD4$^+$ T cells appeared later in the CNS of PI3Kγ$^{-/-}$ mice and their absolute numbers remained lower than in WT mice even at the peak of disease. These findings are fully compatible with combined effects of a deficient migratory capacity of PI3Kγ$^{-/-}$ DCs, which results in delayed T-cell priming [10], and a reduced migratory capacity of PI3Kγ$^{-/-}$ T cells [15].

This concept is further supported by our finding that adoptively transferred PI3Kγ$^{+/+}$ T cells were detectable in the CNS of MOG-immunised PI3Kγ$^{-/-}$ mice several days before their endogenous PI3Kγ$^{-/-}$ T cells. This confirms and extends earlier findings that PI3Kγ controls the migration of Ag-activated CD4$^+$ effector T cells in DTH reaction [15]. Additionally, the lower CD4$^+$ memory survival observed in PI3Kγ$^{-/-}$ mice [39] may contribute to the less severe symptoms observed during the chronic phase.

Our findings may be confounded by the effects of PI3Kγ deficiency in other pathogenetically relevant cell types. PI3Kγ has been extensively involved in leukocyte migration; however, its role in regulating cell migration seems to be different according to the cell type and the chemokine receptor involved. In the absence of PI3Kγ function, the in vitro chemotactic response of neutrophils toward different chemoattractants (IL-8, fMLP and C5a) was severely impaired [11, 14]. In vivo, however, PI3Kγ-independent neutrophil emigration in response to chemokines such as CXCL1 or CXCL2 has also been observed [40, 41].

PI3Kγ deficiency does not affect the expression of TCRαβ, CD3, CD4, CD8, CD28, CD45, CD44, LFA-1, CD25 and CD69 by CD4 or CD8 T cells [14]. In agreement, our in vitro studies showed that PI3Kγ$^{-/-}$CD4$^+$ T cells were able to differentiate into Th0, Th1 or Th17 cells to a similar extent than their WT counterparts. The absence of PI3Kγ expression in BMDC did not affect their capacity to induce Th-cell subset differentiation in vitro. In summary, these results suggest that the delayed T-cell priming and expansion of Ag-specific CD4$^+$ T cells observed in PI3Kγ$^{-/-}$ mice during EAE is not due to an intrinsic defect in T-cell activation, or cytokine production.

Finally, we showed that pharmacological inhibition of PI3Kγ after EAE onset could also influence disease severity. Further studies are required to determine if PI3Kγ could be a therapeutic target for MS.

In summary, here we showed that PI3Kγ contributes to disease severity as well as the time of onset of EAE by acting at different levels. On one hand, the impaired ability of PI3Kγ$^{-/-}$ DCs to migrate delays T-cell priming in the peripheral lymphoid organs. On the other hand, migration defects in PI3Kγ$^{-/-}$ encephalitogenic CD4$^+$ T cells might contribute to the delayed onset and lower severity of disease observed in PI3Kγ-deficient mice.

Materials and methods

Mice

PI3Kγ-deficient (PI3Kγ$^{-/-}$) mice were described earlier [11] and backcrossed to the C57BL/6 background for more than ten generations. WT and PI3Kγ$^{-/-}$ littermates were maintained at the Animal Research Facility, Friedrich Schiller University Jena, Germany and kept under SPF conditions. All animal experiments were approved by the appropriate institutional and governmental committees for animal welfare (02-11-05).

Induction and assessment of EAE

EAE was induced in 8- to 12-wk-old mice by s.c. immunisation with 200 μg MOG peptide, aa35–55 (Peptides&Elephants, Nuthetal, Germany) emulsified in CFA, followed by i.v. injection of 200 ng pertussis toxin (Sigma-Aldrich) on days 0 and 2. To quantify disease severity, scores were assigned daily on a scale of 0–5 as follows: 0, no paralysis; 0.5, clumsy gait; 1, limp tail; 2, limp tail and partial hind leg paralysis; 3, complete hind leg paralysis; 4, tetraparesis and 5, moribund. Animals were euthanised if scores reached grade 4. Treatment with PI3Kγ inhibitor was done as follows: C57BL/6 mice were treated with 30 mg/kg 5-Quinoxalin-6-ylmethylene-thiazolidine-2,4-dione [27] (Calbiochem) i.p., every 12 h for 4 days starting after the onset of clinical symptoms on day 13 pi. In these experiments, scores of 5 were included in the calculation of the mean score for the remainder observation period.

Immunohistochemistry

Sections were stained with H&E or with LFB and periodic acid–Schiff (PAS) reagent for the analysis of inflammation and demyelination. In adjacent serial sections, immunohistochemistry was done with antibodies recognizing macrophages (anti-Mac-3; M3/84; 0781D; BD Pharmingen) or T cells (anti-CD3; CD3-12; MCA 1477; Serotec) as described previously [42]. Bound Ab was visualised by an avidin–biotin technique with diaminobenzidine as the chromogen. Neutrophils were detected by chloracetic esterase histochemistry. Nuclei were counterstained with hematoxylin.

Proliferation and cytokine assays

To determine proliferation, LN or spleen single-cell suspensions were plated in a 96-well round-bottom plate (Greiner Bio-One, Solingen, Germany) at a density of 1×10^6 cells/mL in RPMI1640 culture medium supplemented with 10% FCS, 100 U/mL *penicillin*, 100 μg/mL *streptomycin* and 50 μM 2-mercaptoethanol. Cells were stimulated with 10 μg/mL $MOG_{35–55}$, in triplicate for 72 h. For the last 18 h, 1 μCi/well ^{3}[H]-thymidine (GE Healthcare, München, Germany) was added. ^{3}[H]-thymidine incorporation was measured with a β-scintillation counter. To determine cytokines, supernatants were harvested after 48 h of incubation and analysed for the levels of secreted cytokines using standard sandwich ELISA procedures (IFN-γ was from eBiosciences; IL-17A from R&D Systems).

FACS and mAbs

Unless otherwise indicated, mAbs were grown and purified and/or conjugated from hybridoma supernatants in our laboratory. Single-cell suspensions from dLN (inguinal, para-aortic, 1×10^7 cells/mL) were cultured in 48-well plates in the presence of 30 μg/mL $MOG_{35–55}$ for 5 h. Brefeldin A (Sigma-Aldrich) was added to a final concentration of 5 μg/mL for the last 3 h. Cells were stained with a viability dye (Aqua fixable live/dead staining kit; Invitrogen, Karlsruhe, Germany) according to the manufacturer's instructions. After fixation with 2% paraformaldehyde for 20 min, cells were permeabilised with 0.5% saponin (Sigma-Aldrich) and incubated with anti-CD16/32 (2.4G2/75; 100 μg/mL) and rat IgG (200 μg/mL; Dianova, Hamburg, Germany) to prevent unspecific binding. Cells were stained with anti-CD4 (RM4-5)-APC-A750, IFN-γ (XMG1.2)-PECy7, IL-17A (eBio17B7)-A488, IL-2 (JES6-5H4)-APC and anti-TNF-α (MP6-XT22)-PacBlue all from eBiosciences and anti-CD154 (MR1)-PE purchased from Miltenyi Biotec (Bergisch-Gladbach, Germany); 1 000 000 events were acquired for each sample using a LSRII cell cytometer (BD Biosciences). To determine CNS infiltrates, cell suspensions from the brains and spinal cords were prepared as described previously [36]. Cells were re-stimulated in vitro and analysed by FACS for Ly5.1 (eBiosciences), CD4 and CD154 expression. Gates for CD154 were set using unstimulated control samples as described previously [33]. Alternatively, cells were directly stained with anti-B220(RA3-6B2)-PacBlue, CD4(GK1.5)-Dy495, CD3(145-2C11)-Dy647, NK-T/NK(U5A2-13)-PE (Pharmigen), CD8α (53-6.7)-PECy7 (eBiosciences) or anti-CD11b (M1/70.15.11)-PacBlue, anti-F4/80 (BM8)-PE, anti-Gr1(RB68C5)-APC and anti-CD45 (30-F11)-APC-A750 (eBiosciences) to analyse infiltrating cells. Data were analysed using FlowJo Software (TreeStar, Ashland, OR, USA).

$CD4^+$ Th-cell purification and in vitro stimulation

To prepare BM-derived DCs, BM cells were obtained from the femur and tibia of PI3K$\gamma^{-/-}$ and PI3K$\gamma^{+/+}$ littermates and cultured for 7 days with 10% granulocyte-macrophage-colony-stimulating factor (GM-CSF) supernatant obtained from the Ag8653 myeloma cell line [43]. Naïve $CD4^+CD62L^+$ Th cells were prepared by MACS from spleens and LN using CD4 MultiSort Kit (Miltenyi). A total of 5×10^5 naïve T cells were cultured in the presence of 100 ng/mL LPS (Sigma), 5 μg/mL anti-CD3 and 5×10^4 BMDC under neutral conditions. Th0 cells (without any further cytokines) are induced to differentiate into Th1 cells by supplementation with 5 ng/mL IL-12 (Immunotools) plus 10 μg/mL anti-IL-4 (11B11), or into Th17 cells by supplementation with 10 μg/mL anti-IL-4 (11B11) and 10 μg/mL anti-IFN-γ (XMG 1.2.3.7) plus recombinant mouse IL-6 (20 ng/mL; kind gift of Professor Rose-John, Institute of Biochemistry, University of Kiel) and recombinant human TGF-β1 (2 ng/mL, Preprotech). After 7 days, cells were stimulated in vitro for 4 h with 5 ng/mL PMA and 1 μg/mL ionomycin (Sigma-Aldrich) in the presence of Brefeldin A before being stained for intracellular cytokines. For transfer experiments, total $CD4^+$ cells were purified by MACS and transferred i.p. into PI3K$\gamma^{-/-}$ mice (1×10^7 cells/mouse in 500 μL PBS). In control experiments, PI3K$\gamma^{+/+}$ mice received similarly purified total $CD4^+$ PI3K$\gamma^{-/-}$ Th cells.

Statistical analysis

All data are presented as the mean ± SEM unless otherwise indicated. Statistical analysis (non-parametric Mann–Whitney *U*-test) was performed with SPSS16.0 (SPSS, Chicago, IL, USA) or with GraphPad Prism 5.

Acknowledgements: The authors thank Dr. Emilio Hirsch for kindly providing the PI3K$\gamma^{-/-}$ mice and Dr. Falk Weih for the Ly5.1 congenic mice, the staff of the University hospital's animal facility for excellent animal care and members of our laboratory for their invaluable help. The authors also thank Annett Krause for expert secretarial assistance. This work was supported by grants of the Deutsche Forschungsgemeinschaft (SFB 604 TP C5) to T. K. and J. N., Gemeinnützige Hertie Stiftung (GHS) and Interdisciplinary Centre for Clinical Research (IZKF) 75 to S. H. The present work forms part of the PhD thesis of LB.

Conflict of interest: The authors declare no financial or commercial conflict of interest.

References

1 **Krishnamoorthy, G. and Wekerle, H.,** EAE: an immunologist's magic eye. *Eur. J. Immunol.* 2009. **39**: 2031–2035.

2 **Engelhardt, B.,** Immune cell entry into the central nervous system: involvement of adhesion molecules and chemokines. *J. Neurol. Sci.* 2008. **274**: 23–26.

3 **Goverman, J.,** Autoimmune T cell responses in the central nervous system. *Nat. Rev. Immunol.* 2009. **9**: 393–407.

4 **Hamann, I., Zipp, F. and Infante-Duarte, C.,** Therapeutic targeting of chemokine signaling in Multiple Sclerosis. *J. Neurol. Sci.* 2008. **274**: 31–38.

5 **Stoyanova, S., Bulgarelli-Leva, G., Kirsch, C., Hanck, T., Klinger, R., Wetzker, R. and Wymann, M. P.,** Lipid kinase and protein kinase activities of G-protein-coupled phosphoinositide 3-kinase gamma: structure-activity analysis and interactions with wortmannin. *Biochem. J.* 1997. **324**: 489–495.

6 **Vanhaesebroeck, B. and Waterfield, M. D.,** Signaling by distinct classes of phosphoinositide 3-kinases. *Exp. Cell. Res.* 1999. **253**: 239–254.

7 **Bernstein, H. G., Keilhoff, G., Reiser, M., Freese, S. and Wetzker, R.,** Tissue distribution and subcellular localization of a G-protein activated phosphoinositide 3-kinase. An immunohistochemical study. *Cell. Mol. Biol. (Noisy-le-grand)* 1998. **44**: 973–983.

8 **Li, Z., Jiang, H., Xie, W., Zhang, Z., Smrcka, A. V. and Wu, D.,** Roles of PLC-beta2 and -beta3 and PI3Kgamma in chemoattractant-mediated signal transduction. *Science* 2000. **287**: 1046–1049.

9 **Lopez-Ilasaca, M., Crespo, P., Pellici, P. G., Gutkind, J. S. and Wetzker, R.,** Linkage of G protein-coupled receptors to the MAPK signaling pathway through PI 3-kinase gamma. *Science* 1997. **275**: 394–397.

10 **Del Prete, A., Vermi, W., Dander, E., Otero, K., Barberis, L., Luini, W., Bernasconi, S. et al.,** Defective dendritic cell migration and activation of adaptive immunity in PI3Kgamma-deficient mice. *EMBO J.* 2004. **23**: 3505–3515.

11 **Hirsch, E., Katanaev, V. L., Garlanda, C., Azzolino, O., Pirola, L., Silengo, L., Sozzani, S. et al.,** Central role for G protein-coupled phosphoinositide 3-kinase gamma in inflammation. *Science* 2000. **287**: 1049–1053.

12 **Jones, G. E., Prigmore, E., Calvez, R., Hogan, C., Dunn, G. A., Hirsch, E., Wymann, M. P. et al.,** Requirement for PI 3-kinase gamma in macrophage migration to MCP-1 and CSF-1. *Exp. Cell. Res.* 2003. **290**: 120–131.

13 **Reif, K., Okkenhaug, K., Sasaki, T., Penninger, J. M., Vanhaesebroeck, B. and Cyster, J. G.,** Cutting edge: differential roles for phosphoinositide 3-kinases, p110gamma and p110delta, in lymphocyte chemotaxis and homing. *J. Immunol.* 2004. **173**: 2236–2240.

14 **Sasaki, T., Irie-Sasaki, J., Jones, R. G., Oliveira-dos-Santos, A. J., Stanford, W. L., Bolon, B., Wakeham, A. et al.,** Function of PI3Kgamma in thymocyte development, T cell activation, and neutrophil migration. *Science* 2000. **287**: 1040–1046.

15 **Thomas, M. S., Mitchell, J. S., DeNucci, C. C., Martin, A. L. and Shimizu, Y.,** The p110gamma isoform of phosphatidylinositol 3-kinase regulates migration of effector CD4 T lymphocytes into peripheral inflammatory sites. *J. Leukoc. Biol.* 2008. **84**: 814–823.

16 **Webb, A., Johnson, A., Fortunato, M., Platt, A., Crabbe, T., Christie, M. I., Watt, G. F. et al.,** Evidence for PI-3K-dependent migration of Th17-polarized cells in response to CCR2 and CCR6 agonists. *J. Leukoc. Biol.* 2008. **84**: 1202–1212.

17 **Lehmann, K., Muller, J. P., Schlott, B., Skroblin, P., Barz, D., Norgauer, J. and Wetzker, R.,** PI3Kgamma controls oxidative bursts in neutrophils via interactions with PKCalpha and p47phox. *Biochem. J.* 2009. **419**: 603–610.

18 **Tassi, I., Cella, M., Gilfillan, S., Turnbull, I., Diacovo, T. G., Penninger, J. M. and Colonna, M.,** p110Gamma and p110delta phosphoinositide 3-kinase signaling pathways synergize to control development and functions of murine NK cells. *Immunity* 2007. **27**: 214–227.

19 **Alcazar, I., Marques, M., Kumar, A., Hirsch, E., Wymann, M., Carrera, A. C. and Barber, D. F.,** Phosphoinositide 3-kinase gamma participates in T cell receptor-induced T cell activation. *J. Exp. Med.* 2007. **204**: 2977–2987.

20 **Doukas, J., Eide, L., Stebbins, K., Racanelli-Layton, A., Dellamary, L., Martin, M., Dneprovskaia, E. et al.,** Aerosolized phosphoinositide 3-kinase gamma/delta inhibitor TG100-115 [3-[2,4-diamino-6-(3-hydroxyphenyl)pteridin-7-yl]phenol] as a therapeutic candidate for asthma and chronic obstructive pulmonary disease. *J. Pharmacol. Exp. Ther.* 2009. **328**: 758–765.

21 **Ruckle, T., Schwarz, M. K. and Rommel, C.,** PI3Kgamma inhibition: towards an "aspirin of the 21st century"? *Nat. Rev. Drug Discov.* 2006. **5**: 903–918.

22 **Camps, M., Ruckle, T., Ji, H., Ardissone, V., Rintelen, F., Shaw, J., Ferrandi, C. et al.,** Blockade of PI3Kgamma suppresses joint inflammation and damage in mouse models of rheumatoid arthritis. *Nat. Med.* 2005. **11**: 936–943.

23 **Hayer, S., Pundt, N., Peters, M. A., Wunrau, C., Kuhnel, I., Neugebauer, K., Strietholt, S. et al.,** PI3Kgamma regulates cartilage damage in chronic inflammatory arthritis. *FASEB J.* 2009. **23**: 4288–4298.

24 **Pinho, V., Souza, D. G., Barsante, M. M., Hamer, F. P., De Freitas, M. S., Rossi, A. G. and Teixeira, M. M.,** Phosphoinositide-3 kinases critically regulate the recruitment and survival of eosinophils in vivo: importance for the resolution of allergic inflammation. *J. Leukoc. Biol.* 2005. **77**: 800–810.

25 **Takeda, M., Ito, W., Tanabe, M., Ueki, S., Kato, H., Kihara, J., Tanigai, T. et al.,** Allergic airway hyperresponsiveness, inflammation, and

remodeling do not develop in phosphoinositide 3-kinase gamma-deficient mice. *J. Allergy Clin. Immunol.* 2009. **123**: 805–812.

26 **Thomas, M., Edwards, M. J., Sawicka, E., Duggan, N., Hirsch, E., Wymann, M. P., Owen, C. et al.,** Essential role of phosphoinositide 3-kinase gamma in eosinophil chemotaxis within acute pulmonary inflammation. *Immunology* 2009. **126**: 413–422.

27 **Barber, D. F., Bartolome, A., Hernandez, C., Flores, J. M., Redondo, C., Fernandez-Arias, C., Camps, M. et al.,** PI3Kgamma inhibition blocks glomerulonephritis and extends lifespan in a mouse model of systemic lupus. *Nat. Med.* 2005. **11**: 933–935.

28 **Gukovsky, I., Cheng, J. H., Nam, K. J., Lee, O. T., Lugea, A., Fischer, L., Penninger, J. M. et al.,** Phosphatidylinositide 3-kinase gamma regulates key pathologic responses to cholecystokinin in pancreatic acinar cells. *Gastroenterology* 2004. **126**: 554–566.

29 **Lupia, E., Goffi, A., De Giuli, P., Azzolino, O., Bosco, O., Patrucco, E., Vivaldo, M. C. et al.,** Ablation of phosphoinositide 3-kinase-gamma reduces the severity of acute pancreatitis. *Am. J. Pathol.* 2004. **165**: 2003–2011.

30 **Frey, O., Meisel, J., Hutloff, A., Bonhagen, K., Bruns, L., Kroczek, R. A., Morawietz, L. et al.,** Inducible costimulator (ICOS) blockade inhibits accumulation of polyfunctional T helper 1/T helper 17 cells and mitigates autoimmune arthritis. *Ann. Rheum. Dis.* 2010. **69**: 1495–1501.

31 **Frey, O., Reichel, A., Bonhagen, K., Morawietz, L., Rauchhaus, U. and Kamradt, T.,** Regulatory T cells control the transition from acute into chronic inflammation in glucose-6-phosphate isomerase-induced arthritis. *Ann. Rheum. Dis.* 2010. **69**: 1511–1518.

32 **Chattopadhyay, P. K., Yu, J. and Roederer, M.,** A live-cell assay to detect antigen-specific CD4+ T cells with diverse cytokine profiles. *Nat. Med.* 2005. **11**: 1113–1117.

33 **Frentsch, M., Arbach, O., Kirchhoff, D., Moewes, B., Worm, M., Rothe, M., Scheffold, A. et al.,** Direct access to CD4+ T cells specific for defined antigens according to CD154 expression. *Nat. Med.* 2005. **11**: 1118–1124.

34 **Kirchhoff, D., Frentsch, M., Leclerk, P., Bumann, D., Rausch, S., Hartmann, S., Thiel, A. et al.,** Identification and isolation of murine antigen-reactive T cells according to CD154 expression. *Eur. J. Immunol.* 2007. **37**: 2370–2377.

35 **Meier, S., Stark, R., Frentsch, M. and Thiel, A.,** The influence of different stimulation conditions on the assessment of antigen-induced CD154 expression on CD4+ T cells. *Cytometry A* 2008. **73**: 1035–1042.

36 **Brustle, A., Heink, S., Huber, M., Rosenplanter, C., Stadelmann, C., Yu, P., Arpaia, E. et al.,** The development of inflammatory T(H)-17 cells requires interferon-regulatory factor 4. *Nat. Immunol.* 2007. **8**: 958–966.

37 **Stromnes, I. M., Cerretti, L. M., Liggitt, D., Harris, R. A. and Goverman, J. M.,** Differential regulation of central nervous system autoimmunity by T(H)1 and T(H)17 cells. *Nat. Med.* 2008. **14**: 337–342.

38 **Kent, S. J., Karlik, S. J., Cannon, C., Hines, D. K., Yednock, T. A., Fritz, L. C. and Horner, H. C.,** A monoclonal antibody to alpha 4 integrin suppresses and reverses active experimental allergic encephalomyelitis. *J. Neuroimmunol.* 1995. **58**: 1–10.

39 **Barber, D. F., Bartolome, A., Hernandez, C., Flores, J. M., Fernandez-Arias, C., Rodriguez-Borlado, L., Hirsch, E. et al.,** Class IB-phosphatidylinositol 3-kinase (PI3K) deficiency ameliorates IA-PI3K-induced systemic lupus but not T cell invasion. *J. Immunol.* 2006. **176**: 589–593.

40 **Ferguson, G. J., Milne, L., Kulkarni, S., Sasaki, T., Walker, S., Andrews, S., Crabbe, T. et al.,** PI(3)Kgamma has an important context-dependent role in neutrophil chemokinesis. *Nat. Cell. Biol.* 2007. **9**: 86–91.

41 **Liu, L., Puri, K. D., Penninger, J. M. and Kubes, P.,** Leukocyte PI3Kgamma and PI3Kdelta have temporally distinct roles for leukocyte recruitment in vivo. *Blood* 2007. **110**: 1191–1198.

42 **Nogai, A., Siffrin, V., Bonhagen, K., Pfueller, C. F., Hohnstein, T., Volkmer-Engert, R., Bruck, W. et al.,** Lipopolysaccharide injection induces relapses of experimental autoimmune encephalomyelitis in nontransgenic mice via bystander activation of autoreactive CD4+ cells. *J. Immunol.* 2005. **175**: 959–966.

43 **Zal, T., Volkmann, A. and Stockinger, B.,** Mechanisms of tolerance induction in major histocompatibility complex class II-restricted T cells specific for a blood-borne self-antigen. *J. Exp. Med.* 1994. **180**: 2089–2099.

Abbreviations: **dLN:** draining lymph node · **LFB:** Luxol fast blue · **MOG:** myelin oligodendrocyte glycoprotein · **PAS:** periodic acid–Schiff · **pi:** post-immunisation

Full correspondence: Dr. Thomas Kamradt, Institute for Immunology, University Hospital Jena, Friedrich-Schiller-University Jena, Leutragraben 3, D-07743 Jena, Germany
Fax: +49-36-4193-8782
e-mail: Immunologie@mti.uni-jena.de

Current address: Luciana Berod, Institute of Infection Immunology, TWINCORE/Centre for Experimental and Clinical Infection Research; a joint venture between the Medical School Hannover (MHH) and the Helmholtz Centre for Infection Research (HZI)

Received: 18/3/2010
Revised: 1/11/2010
Accepted: 16/12/2010
Accepted article online: 4/1/2011

